International Core Journal of Engineering Volume 8 Issue 3, 2022
ISSN: 2414-1895 DOI: 10.6919/ICJE.202203_8(3).0018

Fault Identification Method for Flexible DC Distribution Networks based on Time Correlation Coefficients

Dong Li[1,2], Hao Wu[1,2], Yuping Yang[1,2], and Lei Chen[1,2]

[1] School of Automation and Information Engineering, Sichuan University of Science & Engineering, Zigong 643000, China

[2] Sichuan Provincial Key Laboratory of Artificial Intelligence, Zigong 643000, China

Abstract

The fault current component characteristics of the DC lines of the flexible DC distribution network are analysed for faults inside and outside the zone: for faults outside the zone, positive and negative fault current components are positively correlated at both ends of the identification line; for faults inside the zone, negative fault current components are negatively correlated at both ends of the identification line, while positive fault current components are positively correlated at non-fault poles. This paper uses the time correlation coefficient to characterise the similarity of the positive and negative fault current components at both ends of the identification line, and investigates the fault identification method based on the time correlation coefficient. The method uses the positive and negative current signal fault current components at both ends of the line to establish the criteria for fault identification. Simulation verification shows that the method can accurately identify faults and fault poles within and outside the zone, with simple threshold setting, high reliability, good resistance to transition resistance and fault distance adaptability.

Keywords

Flexible DC Distribution Networks; Voltage-sourced Converters; Time-dependent Coefficients; DC Cables; Fault Identification.

1. Introduction

With the continuous development of urbanisation, more and more distributed power sources and DC loads are connected to the urban distribution network, and the traditional AC distribution network can no longer meet the requirements of distributed power sources and DC loads for reliability of power supply and high quality of electricity. At the same time, the rapid development of voltage sourced converters (hereinafter referred to as VSC) has led to widespread interest in flexible DC distribution network technology at home and abroad. Compared with the traditional AC distribution network, flexible DC distribution network has large power supply capacity, low line loss, high power quality, flexible control and easy to accept distributed power sources [1-2]. DC lines have low construction costs and low line losses, but in the event of a fault, the fault current rises quickly and has large peaks, so faults must be identified quickly [3-4]. Among the relevant existing studies: the literature [5] extracts the fault current signal from the discharge circuit via a fault location module and calculates the fault distance as well as the fault resistance, thus enabling fault location. The method requires low sampling frequency, is low cost to implement and has high economic benefits. The fault detection method proposed in the literature [6] performs the localisation calculation directly in the time domain by means of the rate of change of the voltage on the DC side of the VSC. The method is simple to implement, reliable and has good localisation accuracy.

ISSN: 2414-1895 DOI: 10.6919/ICJE.202203_8(3).0018

The literature [7] uses the ratio of the amplitude integral of the transient pre- and counter-wave as an action criterion for fault identification as well as isolation; finally, the fault is selected by the ratio of the sum variance of the two pole voltages to the steady-state voltage. This method has no protection dead zone, high reliability and low construction cost. The literature [8] uses the non-faulty line DC current to simultaneously cross the zero point or neither of the characteristics of the zero point, by detecting the existence of simultaneous line DC current over the zero point phenomenon, to achieve accurate identification of the fault line. The method is highly reliable and can be applied to both radial and circular flexible DC distribution networks. The literature [9] proposes a fault detection method for flexible DC systems based on the high-frequency energy of the fault transient currents, taking advantage of the fact that the high-frequency components of the sound line currents are more attenuated compared to the faulty lines. The method achieves fault detection by extracting the high-frequency components of the current through the Fourier transform and comparing them with the rectification threshold. The method is validated by simulation to have high sensitivity and tolerance to transition resistance. A new method of differential protection based on frequency band distribution is proposed in the literature [10]. The method extracts the high and low frequency energy of the differential current signal through discrete wavelet transform, and identifies internal and external faults through the high and low frequency energy ratio region. The method can realise the whole line of fast-acting protection with high reliability and sensitivity. However, the method can only be used for the detection of bipolar faults. In the literature [11], a Pearson correlation coefficient-based protection method for flexible DC distribution networks is proposed using the correlation of DC voltages as the cut-off point. The method uses the Pearson correlation coefficient to measure the correlation between the positive and negative line terminal voltages on the DC side for the identification of faults in the zone. The disadvantage is that the method can only be used for the identification of single pole faults.

This paper investigates a method for fault identification in flexible DC distribution networks based on the First Order Temporal Correlation Coefficient (TOC) for the similarity of the DC-side fault current components. The method achieves fault detection by detecting the instantaneous value of the current at the dc-side outlet of a voltage-source converter (VSC). If a fault occurs in the detection system, the current signals at both ends of the identification line are extracted within 2ms, and the similarity between the positive and negative pole current signals at both ends of the line is calculated using time correlation coefficients, which are used to differentiate between faults inside and outside the zone and to select the poles of the fault. The proposed algorithm is validated by modeling with PSCAD/EMTDC power simulation software, which allows fault pole selection for single pole earth faults as well as double pole faults and the identification of faults inside and outside the zone.

2. Flexible DC Distribution Network Structure and Fault Current Analysis

2.1 Structure of a Flexible DC Distribution Network

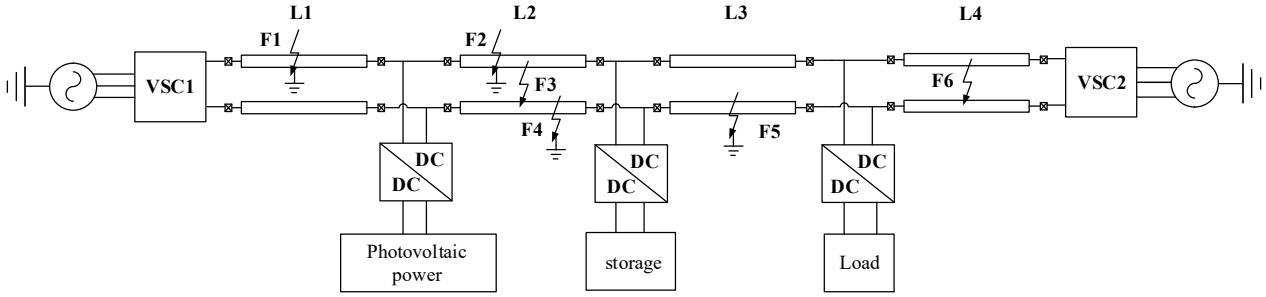

Figure 1. Topology of a flexible DC distribution network

Combining the current domestic and international flexible DC distribution network projects and research results on flexible DC distribution network structures, this paper builds a "hand-in-hand" type medium voltage flexible DC distribution system as shown in Figure 1. The two ends of the

ISSN: 2414-1895 DOI: 10.6919/ICJE.202203_8(3).0018

system are connected to the 110kV AC mains network via 110kV-±10kV voltage source converters VSC1 and VSC2. When one end of the converter is out of service (out of service for maintenance, or out of service in case of fault) or when the middle line is faulty, the non-faulty area can be supplied normally via the converter at the other end. VSC1 and VSC2 both use three-phase two-level voltage source converters with a lower harmonic output and are more economical.

2.2 Fault Current Component Analysis

When the system is in normal operation, the current flows in the same direction at both ends of the line, and under ideal conditions, regardless of line resistance and other external factors, the current at both ends of the line is also equal in magnitude. When a fault occurs in the DC line of the flexible DC distribution system, the circuit superposition principle can be used to analyse the full current of the fault. At this point, the system can be considered as a superposition of two networks before and after the system fault [4,12]. As a result, the fault full current can be expressed as:

$$I_{Fj} = I_{set} + \Delta I_{fj} \tag{1}$$

Where I_{Fj} is the full DC line current after the fault; I_{set} is the DC line positive (or negative) load current during normal operation; ΔI_{fj} is the fault current component; $j = 1,2,3,\ldots,6$ represents the label of each type of fault shown in Figure 1. The fault current component can be obtained through equation (1).

Take the F2 zone positive fault as an example, when the zone occurs positive ground fault, through the formula (1) decomposition to obtain its positive current fault current component, Figure (2) is the relevant current waveform, from top to bottom: positive fault full current waveform, system rated current (positive) waveform and positive fault current component waveform; horizontal coordinate is the number of sampling points; vertical coordinate is the current instantaneous value (in kA).

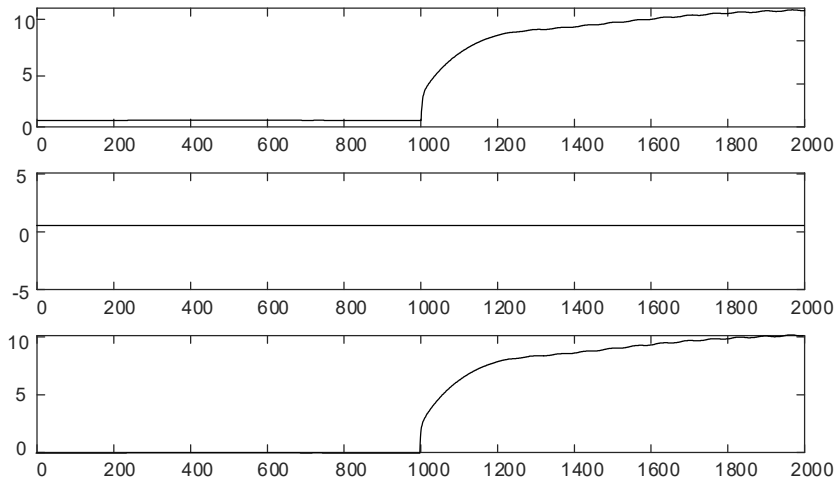

Figure 2. Extraction of fault current components

Literature [13] in the analysis of the fault current components show that: when the system occurs within the fault zone, the fault pole current at both ends of the line fault component polarity opposite, non-fault pole current fault component polarity the same; and when the system occurs outside the zone fault, the fault pole at both ends of the line and non-fault pole current fault component polarity are the same.

Specify the positive direction of current in each section of the line as shown in Figure 3.

ISSN: 2414-1895 DOI: 10.6919/ICJE.202203_8(3).0018

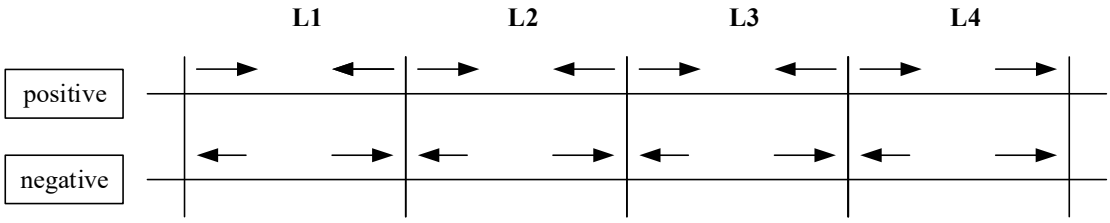

Figure 3. Positive direction of line current for each section of the system in normal operation

2.3 Typical Fault Simulation Analysiss

2.3.1 Simulation Analysis of Typical Faults in the Zone

When a single pole ground fault occurs in the zone, the positive pole single pole ground fault in the F2 zone as an example. Figure 4 shows the positive and negative fault current component waveforms at both ends of L2, from top to bottom: positive fault current component waveform at the left end of L2 line, positive fault current component waveform at the right end of L2 line, negative fault current component waveform at the left end of L2 line, negative fault current component waveform at the right end of L2 line; the horizontal coordinate is the number of sampling points; the vertical coordinate is the instantaneous value of current (in kA).

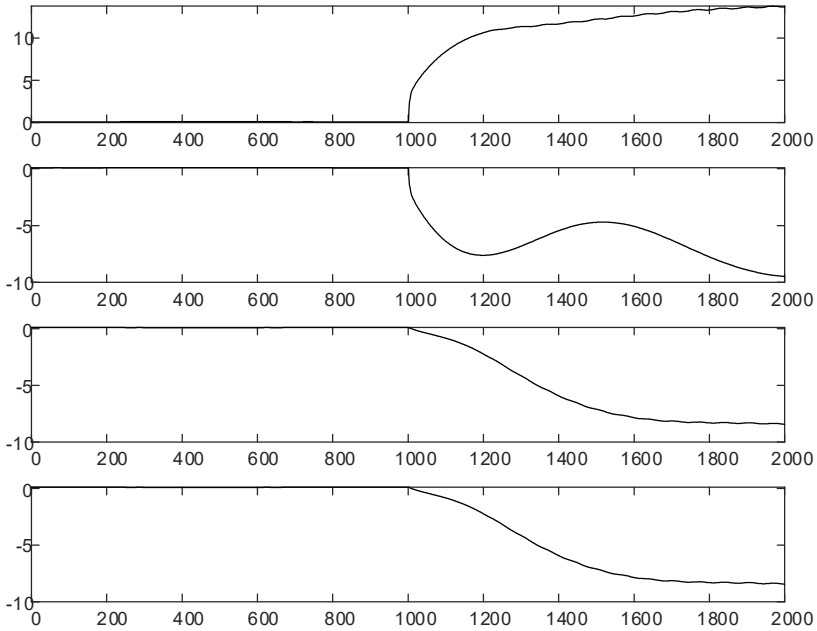

Figure 4. Positive and negative current waveforms at both ends of L2 when F3 fault occurs

When the F2 fault occurs, L2 line left end positive fault current component increases, flow direction and the prescribed positive direction is positive correlation; L2 line right end positive fault current component increases in the opposite direction, flow direction and the prescribed positive direction is negative correlation, line two ends positive fault current component waveform similarity is low. L2 left end negative fault current component increases in the opposite direction, flow direction and the prescribed positive direction is negative correlation; L2 right end negative fault The current component increases in the reverse direction, and the flow direction is negatively correlated with the prescribed positive direction, and the negative pole fault current component waveform at both ends of the line is similar to a higher degree.

When a bipolar fault occurs in the zone, to F4 zone bipolar ground fault as an example. l2 both ends of the positive, negative fault current component waveform shown in Figure 5.

ISSN: 2414-1895 DOI: 10.6919/ICJE.202203_8(3).0018

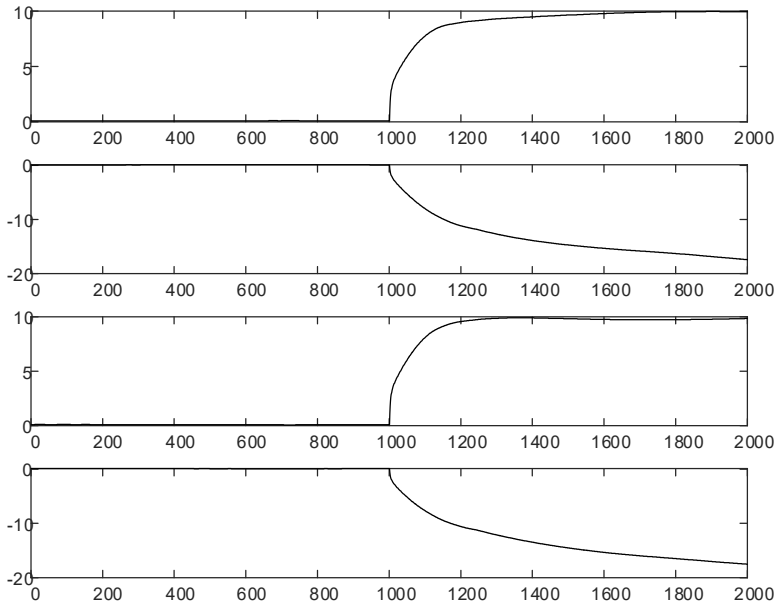

Figure 5. Positive and negative current waveforms at both ends of L2 when F4 fault occurs

When the F4 fault occurs, L2 line left end positive fault current component increases, the flow direction is positively correlated with the prescribed positive direction; L2 line right end positive fault current component increases in reverse, the flow direction is negatively correlated with the prescribed positive direction, the line two ends positive fault current component waveform difference is larger, the similarity is lower. L2 left end negative fault current component increases, the flow direction is positively correlated with the prescribed positive direction; L2 right end negative The fault current component increases in the reverse direction, the flow direction is negatively correlated with the prescribed positive direction, and the negative current signal waveforms at both ends of the line are more different and less similar.

2.3.2 Out-of-area Typical Fault Simulation Analysis

When a positive single pole earth fault occurs outside zone F1. the waveforms of the positive and negative fault currents components at both ends of L2 are shown in Figure 6.

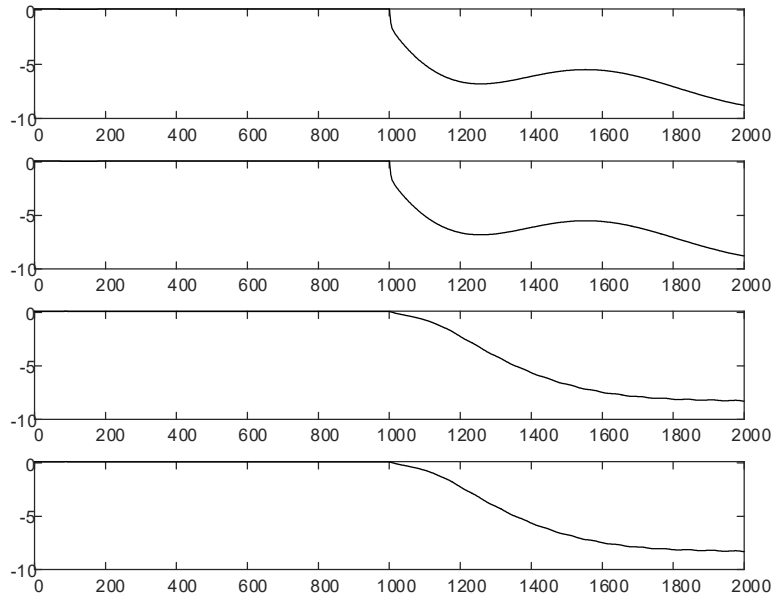

Figure 6. Positive and negative current waveforms at both ends of L2 when F1 fault occurs

ISSN: 2414-1895 DOI: 10.6919/ICJE.202203_8(3).0018

When the F1 fault occurs, the L2 line left end positive fault current component increases in the reverse direction, the flow direction is negatively correlated with the prescribed positive direction; L2 line right end positive fault current component increases in the reverse direction, the flow direction is negatively correlated with the prescribed positive direction, the line two ends of the positive current signal waveform is similar to higher. The negative fault current component at the right end of L2 increases in the opposite direction, and the flow direction is negatively correlated with the prescribed positive direction, and the negative fault current component waveforms at both ends of the line still maintain a high degree of similarity.

When the F6 fault occurs, the positive and negative fault current component waveforms at both ends of L2 are shown in Figure 7.

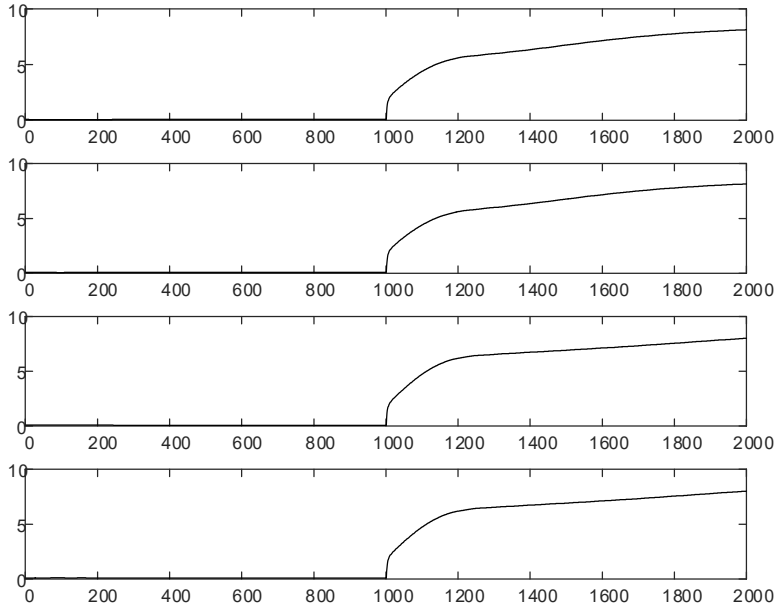

Figure 7. Positive and negative current waveforms at both ends of L2 when F6 fault occurs

When the F6 area outside the bipolar fault occurs, L2 line left end of the positive fault current component increases, the flow direction and the prescribed positive direction is positive correlation; L2 line right end of the positive fault current component increases, the flow direction and the prescribed positive direction is positive correlation, the line two ends of the positive fault current component waveform similarity is higher. L2 left end of the negative current signal increases, the flow direction and the prescribed positive direction is positive correlation; L2 right end of the negative fault current the negative fault current component at the right end of L2 increases, and the flow direction is positively correlated with the prescribed positive direction, and the negative fault current component waveforms at both ends of the line have a higher degree of similarity.

Due to the influence of the fault current component, when the system occurs at different locations, the identification of the line ends of the positive and negative current signal changes are different: when the system occurs within the fault, the line ends of the fault pole fault full current due to the superimposition of the opposite polarity of the fault current component, resulting in differences, while the non-fault pole superimposed crossing current, the two ends of the current signal remains high similarity; and when the system occurs outside the zone fault, the line ends of the fault pole and non-fault pole fault full current are superimposed on the same polarity of the fault current component, the line ends of the positive and negative current signal will maintain a high degree of similarity.

Therefore, the similarity of the current signals at both ends of the line can be considered for in-zone and out-of-zone fault identification on the line.

ISSN: 2414-1895 DOI: 10.6919/ICJE.202203_8(3).0018

3. Fault Identification Method for Flexible and Straight Distribution Networks based on Time Correlation Coefficients

As can be seen from the analysis in Subsection 2, the flexible DC distribution network fault identification algorithm study can be carried out from the perspective of current similarity. The flexible DC distribution network identification method based on the time correlation coefficient studied in this paper characterises the degree of similarity of the fault current components at both ends of the line by means of the time correlation coefficient, following the full current similarity analysis of the DC line faults. The time correlation coefficient is defined as [14]:

$$CORT(X_T, Y_T) = \frac{\sum_{t=1}^{T-1}(x_{t+1} - x_t) * (y_{t+1} - y_t)}{\sqrt{\sum_{t=1}^{T-1}(x_{t+1} - x_t)^2} * \sqrt{\sum_{t=1}^{T-1}(y_{t+1} - y_t)^2}} \tag{2}$$

Where X_T and Y_T represent two time series; x_{t+1} and x_t represent elements in X_T; y_{t+1} and y_t represent elements in Y_T.

This paper uses time correlation coefficients on both ends of the line current signal to calculate the similarity of the construction of internal and external fault identification criteria, the identification of the line L2 left and right ends of the current signal as a time series X_T, Y_T according to formula (2) to calculate the two ends of the line positive and negative current signal time correlation coefficient to obtain formula (3), the definition of $CORT_p(i_{pl}, i_{pr})$ for the identification of the two ends of the line positive current signal time correlation coefficient; $CORT_n(i_{nl}, i_{nr})$ for the identification of the two ends of the line negative current signal time correlation coefficient.

$$\begin{cases} CORT_p(i_{pl}, i_{pr}) = \dfrac{\sum_{t=1}^{t=20}(i_{pl(t+1)} - i_{plt}) * (i_{pr(t+1)} - i_{prt})}{\sqrt{\sum_{t=1}^{t=20}(i_{pl(t+1)} - i_{plt})^2} * \sqrt{\sum_{t=1}^{t=20}(i_{pr(t+1)} - i_{prt})^2}} \\ CORT_n(i_{nl}, i_{nr}) = \dfrac{\sum_{t=1}^{t=20}(i_{nl(t+1)} - i_{nlt}) * (i_{nr(t+1)} - i_{nrt})}{\sqrt{\sum_{t=1}^{t=20}(i_{nl(t+1)} - i_{nlt})^2} * \sqrt{\sum_{t=1}^{t=20}(i_{nr(t+1)} - i_{nrt})^2}} \end{cases} \tag{3}$$

The sampling frequency of this simulation is 10kHz and the sampling time window is 2ms (i.e. 20 sampling points). In equation (2), i_{pl} indicates the positive current measurement at the left end of the identification line, i_{pr} indicates the positive current measurement at the right end of the identification line, i_{nl} indicates the negative current measurement at the left end of the identification line, and i_{nr} indicates the negative current measurement at the right end of the identification line. When the calculated time correlation coefficient is close to 1, the two time series have the same trend, they will rise or fall at the same time; when the calculated time correlation coefficient is close to -1, the two time series have the opposite trend, they will change in opposite ways, this and that; when the calculated time correlation coefficient is close to 0, the lower the correlation between the changes of the two time series.

3.1 Identification Criteria for In-zone and Out-of-zone Faults

From the above analysis can be seen: when the system occurs in the zone fault, identification line fault pole left and right ends of the current will be because of the superimposed fault current and rapid rise and negative correlation, while the non-fault pole left and right ends of the current will be affected by the fault current and rise (or fall) but the change trend is the same still maintain positive correlation. When the system occurs outside the zone fault, identification line positive and negative ends of the

ISSN: 2414-1895 DOI: 10.6919/ICJE.202203_8(3).0018

current signal rise (or fall) the same trend to maintain a positive correlation. Therefore, the identification criteria for in-zone and out-of-zone faults are set as follows:

$$CORT_p(i_{pl}, i_{pr}) < 0 \bigcup CORT_n(i_{nl}, i_{nr}) < 0 \tag{4}$$

When the time correlation coefficient of at least one of the positive or negative current signals at both ends of the identification line is less than 0, it indicates that an in-zone fault has occurred in the system.

3.2 Pole Selection for Faults in the Zone

The literature [16] points out that when different faults occur in the system, the positive and negative current values on the DC side will change differently, and the similarity of the current signals at both ends of the DC line will become poor due to the fault current, so the time correlation coefficients of the positive and negative current signals on the DC side can be used as the fault pole selection criterion, and the pole selection criterion will be set as follows:

$$\begin{cases} CORT_p(i_{pl}, i_{pr}) < 0 \bigcap CORT_n(i_{nl}, i_{nr}) > 0 & \text{Positive pole failure} \\ CORT_p(i_{pl}, i_{pr}) > 0 \bigcap CORT_n(i_{nl}, i_{nr}) < 0 & \text{Negative pole fault} \\ CORT_p(i_{pl}, i_{pr}) < 0 \bigcap CORT_n(i_{nl}, i_{nr}) < 0 & \text{Bipolar fault} \end{cases} \tag{5}$$

3.3 Fault Identification Process

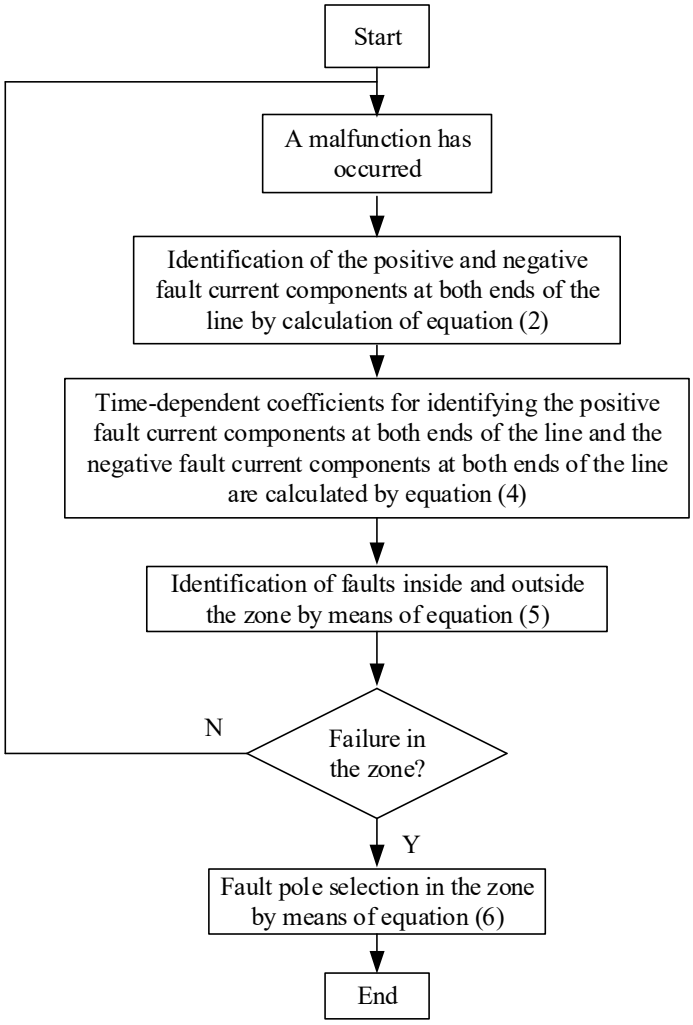

Figure 8. Fault identification process

ISSN: 2414-1895 DOI: 10.6919/ICJE.202203_8(3).0018

The identification process is shown in Figure 8: when the system fault occurs, first according to equation (2) to calculate the positive and negative fault current components at both ends of the line; and then according to equation (4) to calculate the positive fault current component time correlation coefficient at both ends of the line within 2ms and the negative fault current component time correlation coefficient at both ends of the line; followed by equation (5) for in-zone and out-zone fault identification; to confirm the occurrence of in-zone faults then through equation (6) for In-zone fault pole selection. When the fault identification and pole selection criterion is established, identify both sides of the line DC circuit breaker action in tripping.

4. Simulation Analysis

The topology of the simulated flexible DC distribution network model in this paper is shown in Figure 1. The model has an AC side voltage level of 110 kV and a DC side voltage level of , with a simulation sampling frequency of 10 kHz. Typical fault simulation results are shown in Figure 4 to Figure 7.

4.1 Withstand Transition Resistance Test

Table 1. Withstand transition resistance test

Name of fault	Transition resistors	$CORT_p$	$CORT_n$	Discriminating results	Identification results
F1	5Ω	0.8519	0.5953	CORTp>0 CORTn>0	Out-of-zone faults
	10Ω	0.8817	0.5985		
	20Ω	0.8727	0.5716		
F2	5Ω	-0.99519	0.790039	CORTp<0 CORTn>0	In-zone/positive
	10Ω	-0.99905	0.729427		
	20Ω	-0.9934	0.6864		
F3	5Ω	-0.98684	-0.98783	CORTp<0 CORTn<0	In-zone/bipolar
	10Ω	-0.99281	-0.99385		
	20Ω	-0.99725	-0.99826		
F4	5Ω	0.839876	-0.99569	CORTp>0 CORTn<0	In-zone/negative
	10Ω	0.781415	-0.99956		
	20Ω	0.727226	-0.9941		
F5	5Ω	0.753226	0.999482	CORTp>0 CORTn>0	Out-of-zone faults
	10Ω	0.70626	0.999284		
	20Ω	0.658237	0.996923		
F6	5Ω	0.650482	0.651824	CORTp>0 CORTn>0	Out-of-zone faults
	10Ω	0.581465	0.582923		
	20Ω	0.526592	0.52817		

To ensure the accuracy of the measurement results, the measurement start moment is usually set a short time before the fault occurs, with a data window of 2ms (i.e. 20 sampling points). The data obtained after sampling is used to calculate the time correlation coefficient via Matlab to obtain the time correlation coefficient of the positive and negative fault current components at both ends of the line. In this paper, the L2 line is used as the identification line, based on the PSCAD power simulation software for simulation verification (transition resistances are: 5 Ω, 10 Ω and 20 Ω).

ISSN: 2414-1895 DOI: 10.6919/ICJE.202203_8(3).0018

Various fault locations are set up as shown in Figure 1. To test the ability of the proposed protection to withstand the transition resistance, Table 1 shows the positive fault current component time correlation coefficients $CORT_p$ and the negative fault current component time correlation coefficients $CORT_n$ at both ends of the L2 line within 2 ms for different transition resistances from 5 to 20 Ω at each fault location and the identification results.

4.2 Fault Distance Adaptation Analysis

Set the fault location from the left end of the DC line L2 1km, 2km, 3km; set the fault location within the region as shown in Figure 1. To test the adaptability of the proposed identification algorithm to different fault locations, Table 2 shows the fault distance from the left end of the line 1km ~ 3km different fault distance, the positive fault current component time correlation coefficient $CORT_p$ and the negative fault current component time correlation coefficient $CORT_n$ at both ends of the L2 line within 2ms and the identification results.

Table 2. Fault distance adaptation analysis

Name of fault	Fault's distance	$CORT_p$	$CORT_n$	Discriminating results	Identification results
F1	1km	0.980048	0.67943	CORTp>0 CORTn>0	Out-of-zone faults
	2km	0.940669	0.835089		
	3km	0.99689	0.925117		
F2	1km	-0.97877	0.944407	CORTp<0 CORTn>0	In-zone/positive
	2km	-0.98664	0.965138		
	3km	-0.99259	0.965144		
F3	1km	-0.9784	-0.97909	CORTp<0 CORTn<0	In-zone/bipolar
	2km	-0.98144	-0.98226		
	3km	-0.99063	-0.99121		
F4	1km	0.951736	-0.97921	CORTp>0 CORTn<0	In-zone/negative
	2km	0.970837	-0.98721		
	3km	0.968537	-0.9928		
F5	1km	0.954407	0.964787	CORTp>0 CORTn>0	Out-of-zone faults
	2km	0.977862	0.998964		
	3km	0.950194	0.948182		
F6	1km	0.732344	0.733267	CORTp>0 CORTn>0	Out-of-zone faults
	2km	0.743742	0.744802		
	3km	0.760803	0.751428		

4.3 Interference Immunity Analysis

In real engineering, the working environment is more complex than the simulation environment and is full of interference from various signals. To further demonstrate the practicality of the fault identification method, noise disturbances with different signal-to-noise ratios are added to verify the anti-interference capability of the method.

A noise interference with a signal-to-noise ratio of 30db to 50db was set up, and the location of the faults outside the set-up area was shown in Figure 1. To test the adaptability of the proposed

ISSN: 2414-1895 DOI: 10.6919/ICJE.202203_8(3).0018

identification algorithm to different fault locations, Table 3 shows the time correlation coefficients of the positive fault current components $CORT_p$ and the negative fault current components $CORT_n$ at both ends of the L2 line within 2ms and the identification results for different signal-to-noise ratios for faults at F1 to F6.

Table 3. Interference immunity analysis

Name of fault	SNR	$CORT_p$	$CORT_n$	Discriminating results	Identification results
F1	30dB	0.939172	0.129265	CORTp>0 CORTn>0	Out-of-zone faults
	40dB	0.936612	0.656183		
	50dB	0.942858	0.796333		
F2	30dB	-0.98148	0.306635	CORTp<0 CORTn>0	In-zone/positive
	40dB	-0.98702	0.755526		
	50dB	-0.98605	0.955549		
F3	30dB	-0.97542	-0.98206	CORTp<0 CORTn<0	In-zone/bipolar
	40dB	-0.98099	-0.98136		
	50dB	-0.98142	-0.98227		
F4	30dB	0.498966	-0.98513	CORTp>0 CORTn<0	In-zone/negative
	40dB	0.863929	-0.98643		
	50dB	0.938632	-0.9872		
F5	30dB	0.261017	0.994532	CORTp>0 CORTn>0	Out-of-zone faults
	40dB	0.7742	0.998331		
	50dB	0.946776	0.998883		
F6	30dB	0.738374	0.725413	CORTp>0 CORTn>0	Out-of-zone faults
	40dB	0.745109	0.747443		
	50dB	0.740216	0.742845		

4.4 Algorithm Comparison

Table 4. Algorithm comparison

	The algorithm proposed in this paper	Algorithm proposed in the literature [8]	Algorithm proposed in the literature [10]
Maximum transition resistance withstood	20Ω	20Ω	50Ω
With or without recognition dead zone	None	None	None
Tolerable maximum signal-to-noise ratio	30dB	20dB	20dB
Can be used simultaneously for the identification of single and double pole faults inside and outside the zone	Can be used for both single and double pole fault identification inside and outside the zone	Only for the identification of bipolar faults inside and outside the zone	Only for the identification of bipolar faults inside and outside the zone

ISSN: 2414-1895 DOI: 10.6919/ICJE.202203_8(3).0018

A comparison of the fault identification algorithm studied in this paper with other algorithms used for fault identification in flexible DC distribution networks is shown in Table 4.

As can be seen from Table 4, the algorithm proposed in this paper has the same performance compared to the other algorithms in terms of transition resistance tolerance, fault distance adaptability and algorithm time; the advantage over the other two algorithms is that the algorithm proposed in this paper can be used for both single and double pole fault identification; the disadvantage is that the noise interference resistance is weaker than the other two algorithms, and can only tolerate up to 30dB of white noise, while the other Both algorithms can correctly identify faults under the influence of 20dB white noise. This shortcoming will be further improved in subsequent studies.

5. Conclusion

This paper investigates a method for detecting faults on the DC side of a flexible DC distribution network based on time correlation coefficients, which calculates the time correlation coefficients of the positive and negative fault current components at the left end of the identification line for the identification of faults inside and outside the zone and the selection of faults: when a fault occurs outside the identification line, regardless of whether a single pole (positive or negative) earth fault or a When a fault occurs outside the identification line, the positive and negative fault current components will remain positively correlated at both ends of the identification line, regardless of whether a single (positive or negative) earth fault or a double pole fault occurs. When a positive single pole earth fault occurs in the identification line, the fault current components at both ends of the positive DC side of the VSC will be negatively correlated; when a negative single pole earth fault occurs in the identification line, the fault current components at both ends of the negative DC side of the VSC will be negatively correlated; when a double pole fault occurs in the identification line, the fault current components at both ends of the positive and negative DC side of the VSC will be negatively correlated. This allows the identification of faults within and outside the zone and the selection of poles for faults within the zone. The method has been validated through simulation to have the following advantages.

1) selectivity: the identification method enables the identification of faults on the whole line.

2) Reliability: the identification method correctly identifies faults within and outside the zone and has good resistance to noise interference.

3) Sensitivity: the algorithm has a high tolerance to transition resistance and can correctly identify faults with a transition resistance of 20 Ω.

Acknowledgments

This work is supported by National Nature Science Foundation of The Project of Sichuan provincial science and Technology Department (Grant No. 2020YFG0178, 2021YFG0313); The artificial intelligence key laboratory of Sichuan province Foundation (2019RYY01); Graduate Innovation Fund of Sichuan University of Science and Engineering(y2020019).

References

[1] B. BAI, H. CUI, WANG Shuhui, WORDS Ruojia. Current status and outlook of DC distribution grid research [J]. Science and Technology Innovation Herald,2018,15(11):60+62. (In Chinese).

[2] Q. Song, B. Zhao, W.H. Liu, R. Zeng. A review of intelligent DC distribution network research [J]. Chinese Journal of Electrical Engineering,2013,33(25):9-19+5. (In Chinese).

[3] C. F. Dai, X. Y. Liu, M. Huang, et al. Single-pole ground fault protection for ring-shaped flexible and straight distribution network lines based on similarity comparison [J]. Power System Automation, 2019, 43(23): 107-115. (In Chinese).

[4] J.W. He, B. Li, Y. Li, et al. Fast directional longitudinal protection scheme for multi-terminal flexible DC networks [J]. Chinese Journal of Electrical Engineering, 2017, 37(23): 6878-6887. (In Chinese).

ISSN: 2414-1895 DOI: 10.6919/ICJE.202203_8(3).0018

[5] J. Wang, Z.F. Ruan, W. Zhang. Single-end fault location method for flexible DC distribution networks [J]. Information Technology,2020,44(03):125-129. (In Chinese).

[6] M. Zhang, J.H. He, Y.Z. Zhang, G.M. Luo. Fault location method for multi-terminal flexible DC networks [J]. Power Construction,2017,38(08):24-32. (In Chinese).

[7] Z.H. Dai, Z.Q. Liu, M.Y. Yang, X.Y. Liu, L.D. Qin. Longitudinal protection of flexible DC networks based on transient traveling wave amplitude integration [J/OL]. Chinese Journal of Electrical Engineering. (In Chinese).

[8] T. Zheng, Q. Wu, W.X. Lv, X.G. Wang, H. Cao. Research on the protection scheme of flexible DC distribution network based on DC current over zero characteristics [J]. Power Grid Technology, 2020, 44 (05):1806-1815. (In Chinese).

[9] D.S. ZHOU, J.P. LI, Y.J. LI, H.L. BAO, B. SHEN, G.B. SONG. A fault detection method for multi-terminal DC systems based on transient high-frequency energy [J]. Intelligent Power,2019, 47(05): 71-77. (In Chinese).

[10] Li Meng. Research on protection of flexible DC distribution network [D]. Beijing:North China Electric Power University,2018. (In Chinese).

[11] X. Shangguan, W. P. Qin, F. L. Xia, C. G. Ren, J. H. Y. Z. Wang, Liu. A single-pole ground fault protection scheme for MMC multi-terminal flexible DC distribution networks based on transient voltage Pearson correlation [J]. High Voltage Technology, 2020, 46(05): 1740-1749. (In Chinese).

[12] X.J. Wang, H.F. Zhang, X.B. Zhao. Identification and ranging of bipolar short-circuit fault segments in flexible DC distribution networks [J]. Power Supply,2020,37(09):50-57. (In Chinese).

[13] Z.H. Dai, X.Y. Liu, Z.Q. Liu, Y.R. Li, S.Q. Chen. Principles of longitudinal protection for flexible and straight distribution lines based on current fault components [J/OL]. High Voltage Technology. (In Chinese).

[14] Informatioon https://www.heywhale.com/mw/project/603b786304f2500015a12a68.

[15] X.Y. Tong, M.J. Yang, G.S. Zhang. A protection scheme for high-voltage DC transmission lines based on the similarity of traveling waveforms with improved DTW [J]. Chinese Journal of Electrical Engineering, 2020,40(12):3878-3888. (In Chinese).

[16] Y.CZeng, G.B. Zou, C.J. Sun, L.T. Jiang. A DC-side fault protection method for flexible DC distribution networks [J]. Power Information and Communication Technology, 2018, 16(07): 80-86. (In Chinese).

[17] B. JIANG, X.Z. DONG, S.X. SHI. Single-phase ground fault routing method for distribution lines based on single-phase electropop wave[J]. Chinese Journal of Electrical Engineering, 2014, 34(34): 6216-6227. (In Chinese).

[18] H.B. Ge. Research on protection technology of flexible DC distribution network [D]. Hebei: North China Electric Power University,2017. (In Chinese).

[19] J.Y. Liu. Research on fault routing and location method of DC distribution network based on VSC [D]. Hebei: North China Electric Power University,2019. (In Chinese).

[20] P. F. Liu P. C. Huang, A method for locating small current ground fault zones based on dynamic time-bending distance. [J]. Power Grid Technology, 2016, 40(3): 952-957. (In Chinese).

[21] K. JIA, M. LI, T.S. BI, C.B. WANG, H.H. QI, Q.X. YANG. Energy distribution differential protection for flexible DC distribution lines [J]. Power Grid Technology, 2017, 41(09): 3058-3065. (In Chinese).